Eur. Phys. J. D **42**, 1–10 (2007)
DOI: 10.1140/epjd/e2006-00269-9

THE EUROPEAN PHYSICAL JOURNAL D

Quadruply excited beryllium-like atoms – a semiclassical model

N. Simonović[a] and P. Grujić

Institute of Physics, P.O. Box 57, 11000 Belgrade, Serbia

Received 3 October 2006 / Received in final form 31 October 2006
Published online 13 December 2006 –

Abstract. The semiclassical spectrum of quadruply highly excited four-electron atomic systems has been calculated for the plane model of equivalent electrons. The energy of the system consists of rotational and vibrational modes within the circular skeleton orbit approximation, as used in a previous calculation for the triply excited three-electron systems. The full dynamical analysis is carried out within the Hamiltonian theory, accounting for the inertial effects and the complete coupling between different degrees of freedom. Here we present numerical results for energy spectrum of the beryllium atom. The lifetimes of the semiclassical states are estimated via the corresponding Lyapunov exponents. The vibrational modes relative contribution to the energy levels rises with the degree of the Coulombic excitation.

PACS. 31.10.+z Theory of electronic structure, electronic transitions, and chemical binding – 31.15.Gy Semiclassical methods – 31.25.Jf Electron correlation calculations for atoms and ions: excited states

1 Introduction

As the experimental technique is advancing feasibility of multiple excitation of atoms has become a laboratory reality. In a recent paper by Hasegawa et al. [1] multiple photoexcitation of beryllium by the synchrotron radiation has been reported. The so-called hollow atoms with configurations $(2s^2 2p 3s)$ (double excitation) and $(1s 3s^2 3p)$ (triple excitation) have been produced. The next step toward the fourfold excitation is envisaged too, in particular in view that it might be easier to achieve than the lower degree of excitations, as the comparison between oscillator strengths of the twofold and threefold excitations reveals [1].

On the theoretical side, modelling many-electron atoms started from the very beginning of 20th century. As early as in 1904 Nagaoka [2] published his first paper dedicated to what now is known as ring atomic model, with 4 electrons circling around the nucleus. In 1912 Nicholson [3] published his first paper on the same subject too. Those early attempts were aimed at providing models that were to describe ground state properties of real atomic systems. We classify them now as "classical models", accounting for the subsequent development of the theory of microscopic systems, resulting ultimately in Quantum Mechanics. Now we are well aware of the inadequacy of these models based on the notion of the classical trajectory, at least as far as the low-lying atomic states are concerned. But as the semiclassical theory has been developed, it has been appreciated that there is a region where this approach becomes useful and even competitive with more rigorous quantum mechanical calculations. This region corresponds to the highly excited states, where electrons appear well separated in space. The latter property allows for neglecting a number of purely quantum mechanical phenomena, like the exchange effects, as well as of some other short-range interactions, like spin-spin one.

Quantum mechanical description of atomic structure has been successfully applied for not very highly excited few-electron systems. However, as the degree of excitations increases direct application of the quantum mechanical formalism becomes cumbersome (see, e.g. [4,5], due to a large mixing of many states (e.g. [8,9]) and semiclassical calculations turn out more feasible. (For the triply excited lithium see the very recent comprehensive review by Madsen [10]). Semiclassical models appear particularly suitable for those few-electron configurations which possess a high degree of spatial symmetry (e.g. [11]). As the quantum mechanical calculations have shown these symmetrical configurations are gradually attained as the degree of excitation, characterized by the principal quantum number n, rises. In the case of the intrashell quadruple excitations ($2 \leq n \leq 6$), the electrons tend to acquire positions at the vertices of a tetrahedron and a simple Rydberg formula provides a reasonable estimate of the energy spectrum [9]. Very recent calculations by Poulsen and Madsen [12,13] were devoted to finding out possible configurations of the multiply excited atomic systems with two, three, four and six electrons. We mention also recent work by Morishita and Lin [14], where a detailed theoretical study of the tetrahedral s^4 configuration has been carried out.

All these theoretical investigations were concerned with low-lying excited states. Further, they were restricted

[a] e-mail: simonovic@phy.bg.ac.yu

to particular types of underlying classical configurations. In [4,5] it was the frozen-radii approximation, whereas in [9,12–14] the angular degrees of freedom were suppressed. In the case of tetrahedral configuration the latter choice dismisses the semiclassical approach from the start, since it involves fivefold collisions (four electrons passing through the nucleus simultaneously). As is well known even threefold classical collision implies formidable analytical difficulties.

Frozen-radii models appear restricted to large-amplitude oscillatory motion, as proposed as early as in 1920-ies, by Langmuir (see, e.g. [23] and references therein). The semiclassical approach is therefore by necessity restricted to nonzero angular momenta of the electrons. For the classical configurations with single electron orbital momenta quantum numbers high and close to their maximum values electron paths are well approximated by circular orbits. These orbits turn out unstable, what corresponds to the metastable quantum states. By applying standard semiclassical quantization rules, one can evaluate rovibronic energy spectra, as it was done for two and three-electron multiply excited systems [11,18]. Further, by evaluating the corresponding Lyapunov exponents, stability of such configurations can be examined [19] and lifetimes of these periodic orbits can be estimated [21].

The systems under consideration here belong to the so-called small-energy systems, which have been studied extensively for the continuum states [23], in the field of the near-threshold studies (see, e.g. [24] and references therein). That the purely classical approach is justified in the case of small energy particles in the continuum is a consequence of the particular properties of Coulomb interaction, as shown by Wannier in his seminal paper [25]. The case of the classical dynamics applied to highly excited atomic species relies also on the Coulombic interaction and on the so-called correspondence identities [22,26].

The general procedure for calculating semiclassical energies and lifetimes is briefly as follows [11]. One first finds out periodic classical orbits and then applies standard quantization rules to quantize the energy spectrum. In this work we account for the inertial effects, due to the coupling of the rotational (body-fixed) and vibrational motions, neglected in [11]. In the next section we enumerate possible classical models as candidates for the underlying skeleton configurations and carry out calculations for the plane case. In Section 4 the energy spectrum of the beryllium atom is evaluated and in the last section we discuss the results.

2 The semiclassical models

Similarly to the continuum states the first step in establishing the classical model is to set up the skeleton, equilibrium configuration, which corresponds to the so-called leading (scaling) configurations in the near-threshold regime. In the planar case there is a strong analogy between the bound and continuum states symmetry, as the case with the three electron system is [11]. However, moving to three-dimensional configuration this analogy is partially lifted. Namely, the central symmetry present in the free motion case goes into a more restricted symmetry for the bound motion. This is a direct consequence of the change of the active degrees of freedom. In the near-threshold kinematics the main direction is radial one, whereas for the negative energy states it is mainly angular motion that supports the bounded motion (in the quantum mechanical case multiple collisions at nucleus of many electron configurations do not make problem, see, e.g. [9]).

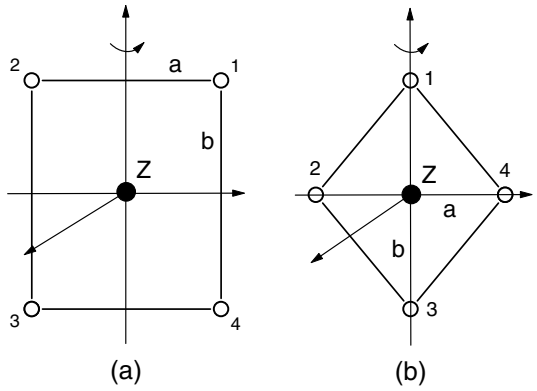

Fig. 1. The skeleton configurations for the rotating-plane models.

In finding the skeleton configuration one first establishes the static one and then finds out dynamical equilibrium state. The most convenient way to examine few-body systems is to make use of the hyperspherical collective coordinates

$$\varphi_{ij} = \angle(\boldsymbol{r}_i, \boldsymbol{r}_j) \quad - \quad \text{mutual angle,} \tag{1}$$

$$\alpha_{i1} = \arctan(r_i/r_1) \quad - \quad \text{hyperangle,} \tag{2}$$

$$R^2 = \sum r_i^2, \quad - \quad \text{hyperradius.} \tag{3}$$

where r_i are radial coordinates of the particles from the centre-of-mass of the entire system.

Generally, to find out the static skeleton configuration one calculates the minimum of the potential function

$$V(\alpha, \varphi, R) = C(\alpha, \varphi)/R, \tag{4}$$

on the hypersphere $R = R_0 = const$. In practice one selects in advance obvious candidates with appropriate symmetry and then examines the corresponding potential functions. In the bounded motion case the static equilibrium configuration may differ considerably from the kinematic skeleton, due to angular (transverse) motion, which is necessary for maintaining dynamic equilibrium.

We shall distinguish two classes of classical configurations, which one may apply semiclassical quantization upon. These are (i) large-amplitude oscillatory (see, e.g. [6]) and (ii) rovibronic configurations. We enumerate here some rovibronic models with a high degree of symmetry. In Figure 1 we show rotating plane models, with electrons situated at the vertices of the tetragons. Figure 1a contains equivalent electrons, whereas in Figure 1b we have the case of two pairs of nonequivalent, stationary and rotating electrons respectively. In Figure 2 we show

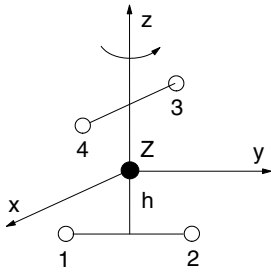

Fig. 2. The skeleton configuration for the rotating-tetrahedral model.

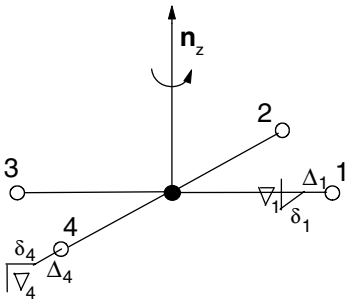

Fig. 3. The skeleton configuration for the planar model, with small deviations from the equilibrium positions.

3D (tetrahedral) rotating model, which turns out to be valid for $Z = 1$ only [20], and thus appears of no physical relevance within our class of rotating skeleton configuration. (Other possible modes of rotation are not excluded, but we have not pursued this possibility here; see, e.g. Fig. 1 in [13], with tetrahedron rotating around Oz-axis.) Thus we restrict ourselves to the tetragonal planar model, with four equivalent electrons rotating around the axis perpendicular to the common plane.

We note that our approach differs from the quantum mechanical models with a fixed radial coordinate, so-called frozen-r approximation (see, e.g. [7]) in that we go beyond the so-called skeleton configuration and account for the vibrational modes.

Regular structures in the few-electron systems indicates correlated motions. These correlations are subjected to stable and unstable modes perturbations. The former are directed transversely to the electron radii, whereas the later are along the radial coordinate. This sort of instability is absent from the molecule-like systems, which are based on different kind of interaction, like Morse potential. Generally, correlations transversely to the radii from the rotation axis are constructive, as opposite to those along the radial distance, which destroy the rotating structure. Within the context of the small-energy systems destructive correlations govern the near-threshold behaviour of a fragmentation function, and in the case of a quasi-bounded motion these instabilities determine the lifetime of the negative-energy systems.

2.1 Beryllium-like planar model

This is an essentially plane tetragonal configuration model, with the nucleus situated at the centre and electrons rotating around the axis perpendicular to the plane. Oscillations around the skeleton equilibrium points are considered, with both stable and unstable modes, as indicated in Figure 3.

As stressed above we consider rovibronic motion as a superposition of rotational and vibrational motions of the equivalent electrons. We find first dynamic equilibrium configurations, by writing first corresponding classical equations for the electrons in the field of an infinitely heavy charge Z.

The Hamilton equations for four electrons moving in the field of an infinitely heavy nucleus of charge Z read

$$\dot{\mathbf{r}}_i = \mathbf{p}_i, \quad \dot{\mathbf{p}}_i = -Z\frac{\mathbf{r}_i}{r_i^3} + \sum_{j(\neq i)}^{1,4} \frac{\mathbf{r}_{ij}}{r_{ij}^3} \equiv \mathbf{F}_i, \quad i = 1,2,3,4. \tag{5}$$

2.1.1 Skeleton configuration

The skeleton configuration for P1 model consists of four electrons rotating with a constant angular velocity Ω in a fixed plane at a fixed distance ρ from the nucleus with mutual angles $\varphi_{ij} = \pi(i-j)/2$ $(i,j = 1,2,3,4)$.

The solution of equations (5) for this configuration is

$$\mathbf{r}_i^{(0)} = \rho\,\hat{n}_\rho^{(i)}, \quad \mathbf{p}_i^{(0)} = \Omega\rho\,\hat{n}_\varphi^{(i)}, \tag{6}$$

where

$$\rho^3 = \frac{Z_{\rm eff}}{\Omega^2} \tag{7}$$

and the effective charge is given by

$$Z_{\rm eff} = Z - \mu_{P1}, \quad \mu_{P1} = \frac{1}{\sqrt{2}} + \frac{1}{4} = 0.95711. \tag{8}$$

The screening parameter μ_{P1} is model dependent.

The unit vectors along $\mathbf{r}_i^{(0)}$ and $\mathbf{p}_i^{(0)}$ directions can be expressed in terms of the unit vectors of the coordinate system $(0,x,y,z)$ in the reference frame rotating with the angular velocity Ω around the z-axis (see Fig. 4)

$$\begin{aligned} \hat{n}_\rho^{(i)} &= c_i\,\hat{n}_x + s_i\,\hat{n}_y, \\ \hat{n}_\varphi^{(i)} &= -s_i\,\hat{n}_x + c_i\,\hat{n}_y, \\ \hat{n}_z^{(i)} &= \hat{n}_z, \end{aligned} \tag{9}$$

where $c_i \equiv \cos\varphi_i$, $s_i \equiv \sin\varphi_i$ and $\varphi_i = \pi(i-1)/2$.

2.1.2 Small deviations from the skeleton configuration

As it is usual within the perturbative approaches one writes the particle positions relative to the origin at the infinitely heavy nucleus with charge Z as

$$\mathbf{r}_i = \mathbf{r}_i^{(0)} + \Delta_i\,\hat{n}_\rho^{(i)} + \delta_i\,\hat{n}_\varphi^{(i)} + \nabla_i\,\hat{n}_z, \tag{10}$$

$$\mathbf{p}_i = \mathbf{p}_i^{(0)} + \Gamma_i\,\hat{n}_\rho^{(i)} + \gamma_i\,\hat{n}_\varphi^{(i)} + \mathrm{L}_i\,\hat{n}_z, \tag{11}$$

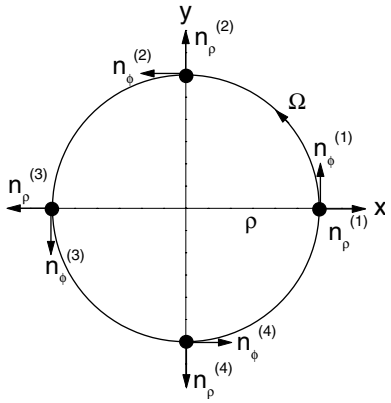

Fig. 4. The skeleton configuration and the unit vectors (9) of electrons local coordinate systems (the third vector $\hat{n}_z$ which is perpendicular to the xy-plane is not shown).

where $\Delta_i, \delta_i, \nabla_i \ll \rho$ (see Fig. 3) and $\Gamma_i, \gamma_i, \mathrm{L}_i \ll \Omega\rho$. Then

$$\dot{\mathbf{r}}_i = \mathbf{p}_i^{(0)} + (\dot{\Delta}_i - \Omega\delta_i)\,\hat{n}_\rho^{(i)} + (\dot{\delta}_i + \Omega\Delta_i)\,\hat{n}_\varphi^{(i)} + \dot{\nabla}_i\,\hat{n}_z, \quad (12)$$

$$\dot{\mathbf{p}}_i = -\Omega^2\mathbf{r}_i^{(0)} + (\dot{\Gamma}_i - \Omega\gamma_i)\,\hat{n}_\rho^{(i)} + (\dot{\gamma}_i + \Omega\Gamma_i)\,\hat{n}_\varphi^{(i)} + \dot{\mathrm{L}}_i\,\hat{n}_z. \quad (13)$$

Using the latest expressions and relations (9) it can be shown that the equations of motion (5) are equivalent to the system of 24 scalar equations for 24 deviations

$$c_i\dot{\Delta}_i - s_i\dot{\delta}_i = s_i\Omega\Delta_i + c_i\Omega\delta_i + c_i\Gamma_i - s_i\gamma_i, \quad (14)$$

$$s_i\dot{\Delta}_i + c_i\dot{\delta}_i = -c_i\Omega\Delta_i + s_i\Omega\delta_i + s_i\Gamma_i + c_i\gamma_i, \quad (15)$$

$$\dot{\nabla}_i = \mathrm{L}_i, \quad (16)$$

$$c_i\dot{\Gamma}_i - s_i\dot{\gamma}_i = c_i\Omega^2\rho + F_x^{(i)} + s_i\Omega\Gamma_i + c_i\Omega\gamma_i, \quad (17)$$

$$s_i\dot{\Gamma}_i + c_i\dot{\gamma}_i = s_i\Omega^2\rho + F_y^{(i)} - c_i\Omega\Gamma_i + s_i\Omega\gamma_i, \quad (18)$$

$$\dot{\mathrm{L}}_i = F_z^{(i)}. \quad (19)$$

After summing equations (14), (15), multiplied at first by c_i and s_i, respectively, and then by $-s_i$ and c_i, and after performing the analogous procedure with equations (17), (18), the system (14–19) transforms to

$$\dot{\Delta}_i = \Omega\,\delta_i + \Gamma_i \quad (20)$$

$$\dot{\delta}_i = -\Omega\,\Delta_i + \gamma_i, \quad (21)$$

$$\dot{\nabla}_i = \mathrm{L}_i, \quad (22)$$

$$\dot{\Gamma}_i = \Omega^2\rho + c_i\,F_x^{(i)} + s_i\,F_y^{(i)} + \Omega\,\gamma_i, \quad (23)$$

$$\dot{\gamma}_i = -s_i\,F_x^{(i)} + c_i\,F_y^{(i)} - \Omega\,\Gamma_i, \quad (24)$$

$$\dot{\mathrm{L}}_i = F_z^{(i)}. \quad (25)$$

2.2 In-plane deviations

Since the deviations ∇_i and L_i do not appear in equations (20), (21), (23), (24), the corresponding system of 16 scalar equations for 16 deviations in plane can be treated separately.

After expanding the force components $F_x^{(i)}$, $F_y^{(i)}$ around the skeleton configuration and keeping only the terms linear in deviations, this system of equations can be written in the 16×16 matrix form

$$\dot{\mathbf{X}} = \mathcal{A}\,\mathbf{X}. \quad (26)$$

Here

$$\mathbf{X} = \{\Delta_1, ..., \Delta_4, \delta_1, ..., \delta_4, \Gamma_1, ..., \Gamma_4, \gamma_1, ..., \gamma_4\} \quad (27)$$

and the 16×16 matrix $\mathcal{A}$ can be given in the block form

$$\mathcal{A} = \begin{Bmatrix} \mathcal{J} & \mathcal{I}_8 \\ \tilde{\mathcal{A}} & \mathcal{J} \end{Bmatrix}, \quad (28)$$

where $\mathcal{I}_n$ is $n \times n$ identity matrix,

$$\mathcal{J} = \Omega \begin{Bmatrix} \mathbf{0} & \mathcal{I}_4 \\ -\mathcal{I}_4 & \mathbf{0} \end{Bmatrix} \quad (29)$$

and

$$\tilde{\mathcal{A}} = \frac{\Omega^2}{Z_{\mathrm{eff}}} \begin{Bmatrix} a & -3b & -\frac{1}{4} & -3b & 0 & -b & 0 & b \\ -3b & a & -3b & -\frac{1}{4} & b & 0 & -b & 0 \\ -\frac{1}{4} & -3b & a & -3b & 0 & b & 0 & -b \\ -3b & -\frac{1}{4} & -3b & a & -b & 0 & b & 0 \\ 0 & b & 0 & -b & c & 3b & \frac{1}{8} & 3b \\ -b & 0 & b & 0 & 3b & c & 3b & \frac{1}{8} \\ 0 & -b & 0 & b & \frac{1}{8} & 3b & c & 3b \\ b & 0 & -b & 0 & 3b & \frac{1}{8} & 3b & c \end{Bmatrix}, \quad (30)$$

where $a = 2Z - (\sqrt{2}+1)/4$, $b = \sqrt{2}/8$, $c = -Z + 1/8 - \sqrt{2}/4$.

To solve (26) one can follow the standard procedure from the theory of small oscillations (see e.g. [30]). Multiplying equation (26) by an unitary matrix $\mathcal{U}$ from the left it transforms into

$$\dot{\mathbf{Z}} = \mathcal{U}\,\mathcal{A}\mathcal{U}^{-1}\mathbf{Z}, \quad \mathbf{Z} \equiv \mathcal{U}\,\mathbf{X}. \quad (31)$$

Now, we choose $\mathcal{U}$ such that

$$\Lambda = \mathcal{U}\,\mathcal{A}\mathcal{U}^{-1} \quad (32)$$

is a diagonal matrix. For the Hamiltonian systems the diagonal elements of Λ (i.e. the eigenvalues of dynamical matrix $\mathcal{A}$) come in the pairs of opposite signs, $\pm\lambda_k$, $k = 1, ..., 8$ (see e.g. [27]). Then (31) reads

$$\dot{\mathbf{Z}} = \Lambda\,\mathbf{Z} \quad (33)$$

which is equivalent to 16 scalar equations

$$\dot{Z}_{2k-1} = \lambda_k Z_{2k-1}, \quad \dot{Z}_{2k} = -\lambda_k Z_{2k}, \quad k = 1, ..., 8, \quad (34)$$

Table 1. The eigenvalues λ_k of the dynamical matrix ($Z = 4$) for deviations in plane and the corresponding eigenvectors $\mathbf{X}^{(n)}$ at $t = 0$ (here $n = 2k - (1 \pm 1)/2$).

k (n)	1 (1, 2)	2 (3, 4)	3 (5, 6)	4 (7, 8)	5 (9, 10)	6 (11, 12)	7, 8 (13, 14, 15, 16)
$\pm\lambda_k/\Omega$	0	$\pm i$	$\pm 1.47699i$	$\pm 1.41658i$	$\pm 1.23955i$	± 1.08697	$(\pm)0.928209 \pm 0.088515i$
$\Delta_1^{(n)}(0)$	0	$\mp 0.188982i$	$\mp 0.166809i$	$\mp 0.183367i$	$\pm 0.165836i$	0.183287	$(\mp)0.003361 \pm 0.169239i$
$\Delta_2^{(n)}(0)$	0	$\mp 0.188982i$	$\pm 0.166809i$	-0.183367	-0.165836	-0.183287	$-0.169239 \pm (\mp)0.003361i$
$\Delta_3^{(n)}(0)$	0	$\mp 0.188982i$	$\mp 0.166809i$	$\pm 0.183367i$	$\mp 0.165836i$	0.183287	$(\pm)0.003361 \mp 0.169239i$
$\Delta_4^{(n)}(0)$	0	$\mp 0.188982i$	$\pm 0.166809i$	0.183367	0.165836	-0.183287	$0.169239 \mp (\mp)0.003361i$
$\delta_1^{(n)}(0)$	∓ 0.353553	0.377964	0.331963	0.343164	-0.35438	∓ 0.212097	$-0.018100 \pm (\mp)0.242123i$
$\delta_2^{(n)}(0)$	∓ 0.353553	0.377964	-0.331963	$\mp 0.343164i$	$\pm 0.35438i$	± 0.212097	$(\pm)0.242123 \mp 0.018100i$
$\delta_3^{(n)}(0)$	∓ 0.353553	0.377964	0.331963	-0.343164	0.35438	∓ 0.212097	$0.018100 \mp (\mp)0.242123i$
$\delta_4^{(n)}(0)$	∓ 0.353553	0.377964	-0.331963	$\pm 0.343164i$	$\pm 0.35438i$	± 0.212097	$(\mp)0.242123 \pm 0.018100i$
$\Gamma_1^{(n)}(0)$	± 0.353553	-0.188982	-0.085588	-0.083411	0.148819	± 0.411324	$\mp(\mp)0.398915i$
$\Gamma_1^{(n)}(0)$	± 0.353553	-0.188982	0.085588	$\pm 0.083411i$	$\pm 0.148819i$	∓ 0.411324	$(\mp)0.398915$
$\Gamma_1^{(n)}(0)$	± 0.353553	-0.188982	-0.085588	0.083411	-0.148819	± 0.411324	$\pm(\mp)0.398915i$
$\Gamma_1^{(n)}(0)$	± 0.353553	-0.188982	0.0855877	$\mp 0.0834108i$	$\mp 0.148819i$	∓ 0.411324	$(\pm)0.398915$
$\gamma_1^{(n)}(0)$	0	$\pm 0.188982i$	$\pm 0.323496i$	$\pm 0.30275i$	$\mp 0.273434i$	-0.047256	$(\pm)0.001269 \mp 0.057105i$
$\gamma_1^{(n)}(0)$	0	$\pm 0.188982i$	$\mp 0.323496i$	0.30275	0.273434	0.047256	$0.057105 \mp (\mp)0.001269i$
$\gamma_1^{(n)}(0)$	0	$\pm 0.188982i$	$\pm 0.323496i$	$\mp 0.30275i$	$\pm 0.273434i$	-0.047256	$(\mp)0.001269 \pm 0.057105i$
$\gamma_1^{(n)}(0)$	0	$\pm 0.188982i$	$\mp 0.323496i$	-0.30275	-0.273434	0.047256	$-0.057105 \pm (\mp)0.001269i$

where $\mathbf{Z} = \{Z_1, ..., Z_{16}\}$. The solutions of (34) are

$$Z_{2k+1} = C_{2k+1} e^{\lambda_k t}, \quad Z_{2k} = C_{2k} e^{-\lambda_k t}, \tag{35}$$

where C_n are arbitrary constants. To return to the original X-space, we have from (31)

$$\mathbf{X} = \mathcal{U}^{-1}\mathbf{Z}. \tag{36}$$

The dynamics around the equilibrium (skeleton configuration) depends exclusively on the eigenvalues $\pm\lambda_k$. The normal modes of the system are related to the eigenvectors $\mathbf{Z}^{(n)} = \{Z_1^{(n)}, ..., Z_{16}^{(n)}\}$, where $Z_{n'}^{(n)}$ are given by (35) with

$$C_{n'}^{(n)} = \delta_{nn'}. \tag{37}$$

Then, in agreement with (36), the corresponding eigenvectors $\mathbf{X}^{(n)}$ coincide to the columns of $\mathcal{U}^{-1}$ multiplied by the exponential factors $e^{\pm\lambda_k t}$, where $n = 2k-1$ stands for $+\lambda_k$ and $n = 2k$ for $-\lambda_k$.

2.3 Off-plane deviations

The system of equations (16), (19), after linearizing the force components $F_z^{(i)}$, can be written in the 8×8 matrix form

$$\dot{\mathbf{Y}} = \mathcal{B}\,\mathbf{Y}. \tag{38}$$

Here

$$\mathbf{Y} = \{\nabla_1, ..., \nabla_4, \mathrm{L}_1, ..., \mathrm{L}_4\} \tag{39}$$

and 8×8 matrix $\mathcal{B}$ can be given in the block form

$$\mathcal{B} = \begin{Bmatrix} \mathbf{0} & \mathcal{I}_4 \\ \tilde{\mathcal{B}} & \mathbf{0} \end{Bmatrix}, \tag{40}$$

where

$$\tilde{\mathcal{B}} = -\frac{\Omega^2}{Z_{\mathrm{eff}}} \begin{Bmatrix} \alpha & \beta^2 & \beta & \beta^2 \\ \beta^2 & \alpha & \beta^2 & \beta \\ \beta & \beta^2 & \alpha & \beta^2 \\ \beta^2 & \beta & \beta^2 & \alpha \end{Bmatrix} \tag{41}$$

and $\alpha = Z - 1/8 - \sqrt{2}/2$, $\beta = 1/\sqrt{8}$.

The eigenvalues of the matrix $\tilde{\mathcal{B}}$ are in the same time the squares of eigenvalues of the matrix $\mathcal{B}$: $\lambda_{1,2,3,4}^2 = -\Omega^2$, $-\Omega^2$, $-\Omega^2\, Z/Z_{\mathrm{eff}}$, $-\Omega^2\,(Z - \sqrt{2})/Z_{\mathrm{eff}}$. For $Z > \sqrt{2}$ all λ^2 are negative and the eigenvalues of $\mathcal{B}$ are purely imaginary, i.e. the off-plane deviations are stable. Then, the eigenvectors of $\tilde{\mathcal{B}}$

$$\begin{aligned} \mathbf{Q}^{(1)} &= \{-1, 0, 1, 0\}, & \mathbf{Q}^{(2)} &= \{0, -1, 0, 1\}, \\ \mathbf{Q}^{(3)} &= \{-1, 1, -1, 1\}, & \mathbf{Q}^{(4)} &= \{1, 1, 1, 1\}, \end{aligned} \tag{42}$$

where $\mathbf{Q}^{(k)} \sim \{\nabla_1^{(k)}(0), \nabla_2^{(k)}(0), \nabla_3^{(k)}(0), \nabla_4^{(k)}(0)\}$, determine the corresponding normal modes of the off-plane small oscillations around the skeleton configuration.

3 Numerical results – beryllium ($Z = 4$)

Among 16 eigenvalues of the dynamical matrix (for deviations in plane), beside the pair of zeros, there are four pairs with purely imaginary values of the opposite signs (stable oscillatory modes), a pair of real eigenvalues (unstable mode) and a quartet of complex eigenvalues (coupled unstable and oscillatory modes), see Table 1. The latest type of eigenvalues may appear only in the systems with more than two degrees of freedom [27].

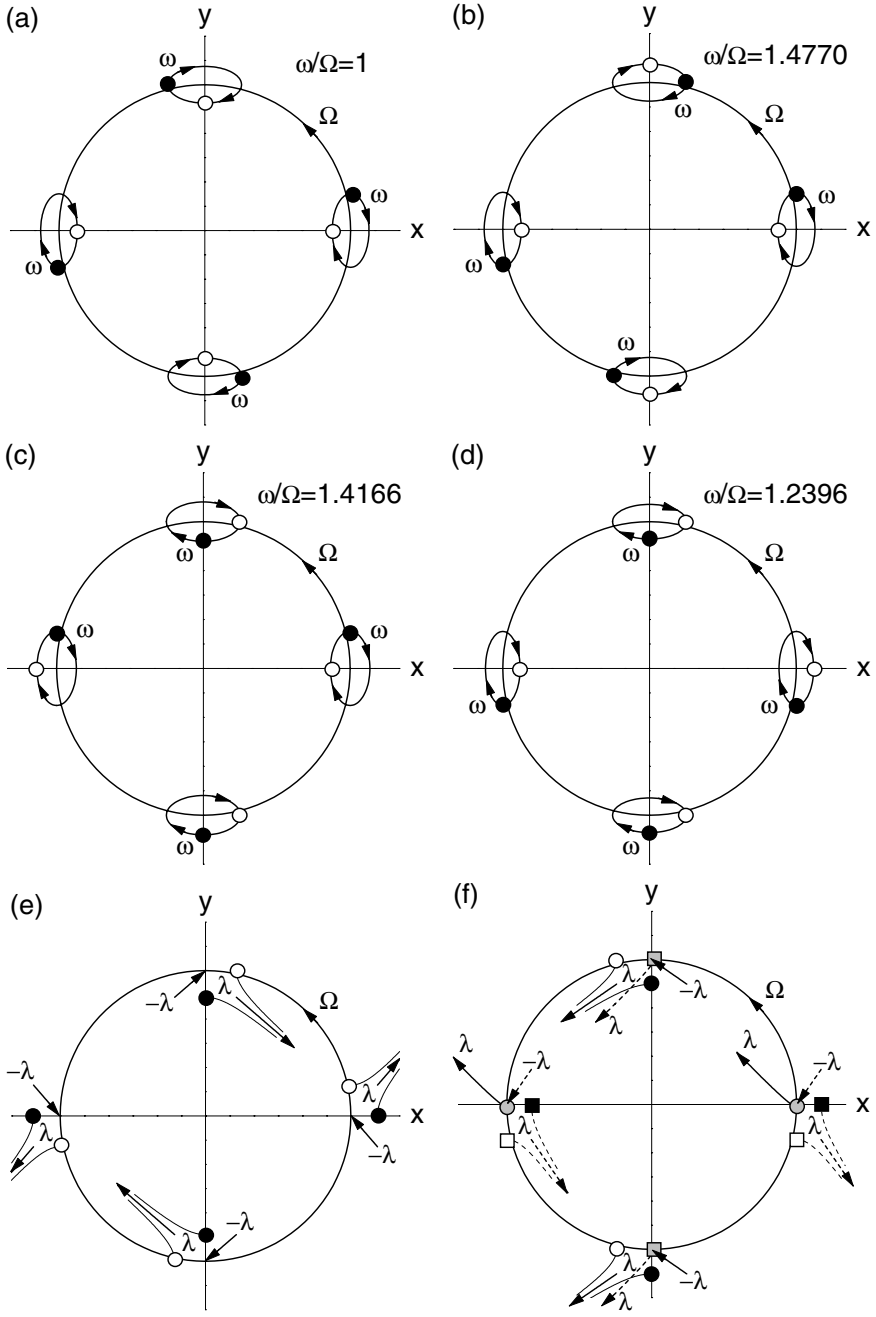

Fig. 5. Stable (a–d) and unstable (e, f) normal modes of small deviations from the skeleton configuration for $Z = 4$. The circles show the positions of electrons with deviations determined by the vectors $\mathbf{X}_{\pm}^{(k)}$ at $t = 0$ (the full/open circles correspond to $+/-$ sign).

The deviations related to the eigenvalue $\lambda = 0$ (see the eigenvectors $\mathbf{X}^{(1,2)}$ whose components are given in the column $k = 1$ in Tab. 1) introduce only a rotational shift and do not change the skeleton configuration essentially.

In the analysis of oscillatory modes ($\lambda_k = i\,\omega_k$, $k = 2, ..., 5$) it is convenient to consider the linear combinations

$$\mathbf{X}_{+}^{(k)} = \frac{\mathbf{X}^{(2k-1)} + \mathbf{X}^{(2k)}}{2}, \quad \mathbf{X}_{-}^{(k)} = \frac{\mathbf{X}^{(2k-1)} - \mathbf{X}^{(2k)}}{2i}, \quad (43)$$

whose components are real in contrast to those of the eigenvectors $\mathbf{X}^{(n)}$ ($n = 3, ..., 10$). For example the eigenvectors $\mathbf{X}^{(3,4)} \equiv \mathbf{X}^{(3,4)}(0) \exp\{\pm i\Omega\, t\}$ (see Tab. 1) give

$$\mathbf{X}_{+}^{(2)} = \frac{1}{2\sqrt{7}}\{\sin\Omega t, ..., \sin\Omega t, 2\cos\Omega t, ..., 2\cos\Omega t, ...\},$$
$$\mathbf{X}_{-}^{(2)} = \frac{1}{2\sqrt{7}}\{-\cos\Omega t, ..., -\cos\Omega t, 2\sin\Omega t, ..., 2\sin\Omega t, ...\}. \quad (44)$$

The evolution of deviations Δ_i, δ_i which are components of the vectors $\mathbf{X}_{\pm}^{(k)}$, $k = 2, ..., 5$, are shown in Figures 5a–5d. The electron trajectories corresponding to the modes $k = 2, 3$ are shown in Figure 6 in the laboratory frame.

Analogously in Figure 5e, beside the stable (λ) and unstable ($-\lambda$) manifolds of the $k = 6$ mode represented

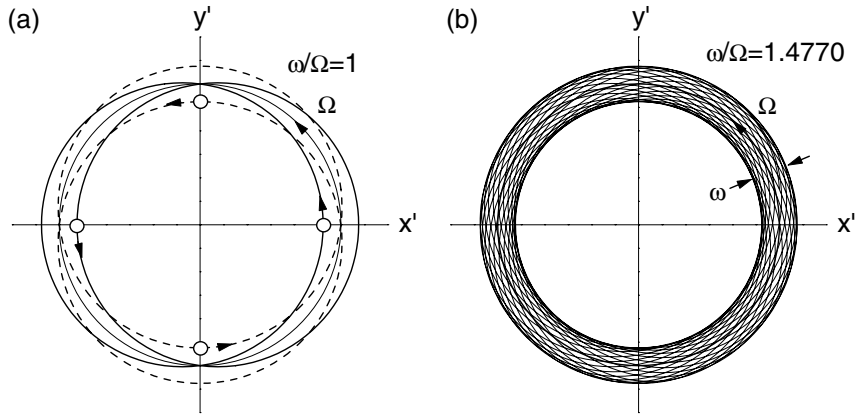

Fig. 6. The electrons trajectories corresponding to the modes from Figures 5a and 5b shown in the laboratory frame.

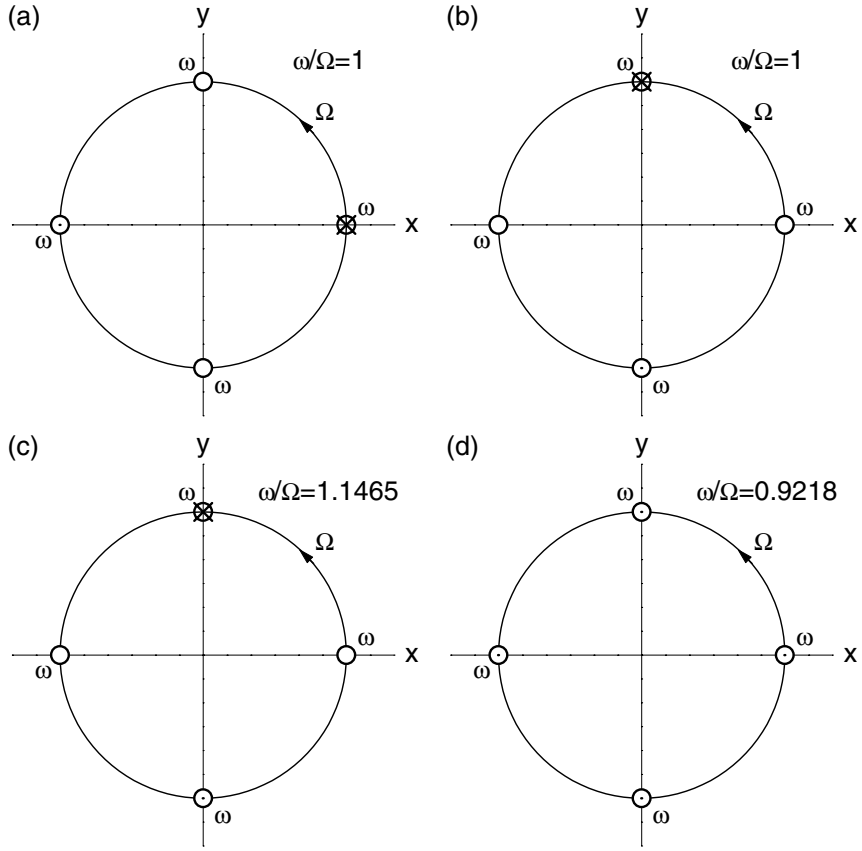

Fig. 7. The off-plane small collective oscillations (normal modes $\mathbf{Q}^{(k)}$ for the case $Z = 4$. The circles show the simultaneous positions of electrons in the xy-plane. The open circles correspond to non-oscillating electrons, whereas the symbols $\odot/\otimes$ denote different phases of oscillations (the up/down directions).

by the vectors $\mathbf{X}^{(11)}$ and $\mathbf{X}^{(12)}$, respectively, the evolution of deviations which are components of the vectors

$$\mathbf{X}_{+}^{(6)} = \frac{\mathbf{X}^{(11)}+\mathbf{X}^{(12)}}{2}, \quad \mathbf{X}_{-}^{(6)} = \frac{\mathbf{X}^{(11)}-\mathbf{X}^{(12)}}{2} \qquad (45)$$

are shown.

For the complex case (Fig. 5f) two stable (λ) and two unstable ($-\lambda$) manifolds are obtained applying equations (43) to the eigenvectors with complex-conjugate components (since $\mathrm{Im}\,\lambda \ll \mathrm{Re}\,\lambda$ the oscillatory part is negligible). Finally, the corresponding pairs of new vectors (now with real components), proportional to the factors $\exp\{\pm\lambda t\}$, are combined once again using (45). The four symbols in Figure 5f (full/open circles and squares) represent the initial positions of electrons leaving the skeleton configuration along the trajectories determined by the latest combinations (the modes represented by full/open symbols of the same type are obtained using the same pair of vectors with $\pm\lambda$). The gray symbols are used in the cases when the initial positions of an electron for the modes represented by full and open symbols almost coincide.

The frequency ratios ω_k/Ω of the off-plane small collective oscillations (normal modes (42), see Fig. 7) for the case $Z = 4$ are: 1, 1, 1.14653, 0.921835.

4 Semiclassical quantization

We divide the quantization procedure into two consecutive steps, starting with the zero-order rigid-rotor model.

4.1 The rigid-rotor approximation

The energy of the skeleton configuration is given by

$$E = -2\frac{Z_{\rm eff}}{\rho}. \tag{46}$$

Since $\rho^3 = Z_{\rm eff}/\Omega$ and, on the other hand, the single electron angular momentum is $l_{\rm e} = \Omega\rho$, one has $\rho = l_{\rm e}^2/Z_{\rm eff}$ and

$$E = -2\frac{Z_{\rm eff}^2}{l_{\rm e}^2} = -32\frac{Z_{\rm eff}^2}{\mathcal{L}^2}, \tag{47}$$

where $\mathcal{L} = 4l_{\rm e}$ is the total angular momentum. Then, the quantization condition

$$\mathcal{L} = L + \frac{1}{2}, \quad L = 0, 1, 2, ... \tag{48}$$

gives the energy spectrum of the four electron system within the rigid rotor approximation

$$E^{(0)} = -32\frac{Z_{\rm eff}^2}{(L+\frac{1}{2})^2}. \tag{49}$$

4.2 Ro-vibrational spectrum

A consequence of the scaling properties of Coulomb systems is that the product I^2E, where $I = S/2\pi$ is an action variable, is invariant under the scaling (similarity) transformations. Then, the energy of a (quasi)periodic configuration (orbit) can be determined if we know the action integral I along the orbit for one (principal) period $2\pi/\Omega$, using the formula

$$E = -\frac{I_{\rm sc}^2}{I^2}, \tag{50}$$

where $I_{\rm sc}$ is the corresponding action at the scaled energy $E_{\rm sc} = -1$. Using simple WKB quantization of the orbit, semiclassical energies follow from the condition

$$I = L + \frac{1}{2} + \sum_k \frac{\omega_k}{\Omega}\left(n_k + \frac{1}{2}\right), \tag{51}$$

where $n_k = 0, 1, 2, ...$ are the vibrational quantum numbers for small oscillations of the stable modes ($\lambda_k = i\omega_k$) in the vicinity of skeleton configuration ($n_k \ll L$). By comparing equations (50), (51) with the formula (49) it is clear that $I_{\rm sc}^2 = -32Z_{\rm eff}^2$ and the semiclassical ro-vibrational spectrum can be obtained using the formula

$$E = -32\frac{Z_{\rm eff}^2}{I^2} \tag{52}$$

together with the condition (51).

The quantization condition (51) does not take into account the unstable modes which may determine the life-times of quantum states. For a correct semiclassical quantization of an unstable system one needs usually to calculate the sum of contributions of all periodic orbits (e.g. using the Gutzwiller trace formula). It is shown, however, that in the cases when only one periodic orbit exists the condition (51) can be extended by including unstable modes, too [32]. The frequencies corresponding to unstable modes are pure imaginary, $\omega_k = -i\lambda_k$, and the action becomes a complex variable. As a consequence the energies are also complex, whose imaginary parts determine decay widths. There are same indications that this approach may be used to estimate the widths of decaying states when a classical configuration is essentially related to a part of energy spectrum, although this configuration might not be the only existing [33]. We shall use this approach to estimate the positions and widths of symmetric highly excited states of beryllium related to the proposed classical configuration.

4.3 The results for beryllium (Z = 4)

As we have seen from the stability analysis of the case $Z = 4$ there are nine stable modes — five in-plane and four off-plane collective oscillatory modes. Since for three of them (e.g. $j = 6, 7, 8$) the winding numbers ω_j/Ω are 1 and for one mode (e.g. $j = 9$) it is 0, the condition (51) reduces to

$$I = N + 2 + \sum_{j=1}^{5} \frac{\omega_j}{\Omega}\left(n_j + \frac{1}{2}\right), \quad N = 0, 1, 2, ..., \tag{53}$$

where $N = L + n_6 + n_7 + n_8$. The winding numbers ω_j/Ω different from 1 ($j = 1, ..., 5$) are: 1.47699, 1.41658, 1.23955, 1.14653, 0.921835, respectively.

If we include the unstable modes, the corresponding complex action variable $\tilde{I}$ is

$$\tilde{I} = I - i\sum_{j=10}^{12} \frac{\lambda_j}{\Omega}\left(n_j + \frac{1}{2}\right), \tag{54}$$

where the ratios λ_j/Ω for unstable modes ($j = 10, 11, 12$) are: $1.08697, 0.928209 \pm 0.088515i$, respectively. The latest two modes with the complex-conjugate exponents are not typical for low dimensional systems, but since $\mathrm{Im}\,\lambda \ll \mathrm{Re}\,\lambda$ we have neglected the imaginary parts.

We shell consider decaying states (resonances) closest to the real energy axis, which are related to the quantum numbers $n_{10} = n_{11} = n_{12} = 0$ (higher values of these quantum numbers are related to broad resonances which form a smooth background of energy spectrum). Then, in this case

$$\mathrm{Im}\,\tilde{I} = -\frac{1}{2}\sum_{j=10}^{12} \frac{\mathrm{Re}\,\lambda_j}{\Omega} = -1.47169. \tag{55}$$

Now, if we extend the formula (52) to complex variables it follows

$$\tilde{E} = -32\frac{Z_{\rm eff}^2}{\tilde{I}^2} = E\left(1+\frac{\operatorname{Im}\tilde{I}}{I}\right)^{-2}, \qquad (56)$$

where $E \equiv \operatorname{Re}\tilde{E}$. Further, for highly excited states $|\operatorname{Im}\tilde{I}| \ll I$ and $\tilde{E} \approx E\,(1-2\operatorname{Im}\tilde{I}/I)$. Then, the widths $\Gamma \equiv -2\operatorname{Im}\tilde{\rm E}$ of these states are

$$\Gamma \approx 4E\frac{\operatorname{Im}\tilde{I}}{I} = \frac{|\operatorname{Im}\tilde{I}|}{\sqrt{2}\,Z_{\rm eff}}\,(-E)^{3/2} \approx 0.342\,(-E)^{3/2}. \qquad (57)$$

We see that the stability of the orbits increases as the continuum is approached, what appears the common feature of the semiclassical theory. Generally one has

$$\Gamma \sim \frac{1}{N^3}, \qquad (58)$$

where N is an effective principal quantum number.

In order to elaborate the connection between the lifetimes $\tau = \hbar/\Gamma$ and Lyapunov exponents of the classical configuration note that $\lambda_j/\Omega = \lambda_j^{(\rm sc)}/\Omega_{\rm sc}$. In fact $\Omega = \Omega_{\rm sc}(-E)^{-3/2}$ and $\lambda = \lambda_{\rm sc}(-E)^{-3/2}$ for $E_{\rm sc} = -1$ [32]. On the other hand, from equations (46) and (7) it follows $\rho_{\rm sc} = 2Z_{\rm eff}$ and $\Omega_{\rm sc} = 1/2\sqrt{2}\,Z_{\rm eff}$. Then, equation (55) can be written in the form

$$\operatorname{Im}\tilde{I} = -\frac{1}{2}\sum_{j=10}^{12}\frac{\operatorname{Re}\lambda_j^{(\rm sc)}}{\Omega_{\rm sc}} = -\sqrt{2}\,Z_{\rm eff}\sum_{j=10}^{12}\operatorname{Re}\lambda_j^{(\rm sc)} \qquad (59)$$

and equation (57) reduces to

$$\Gamma \approx \sum_{j=10}^{12}\operatorname{Re}\lambda_j^{(\rm sc)}\,(-E)^{3/2} = \sum_{j=10}^{12}\operatorname{Re}\lambda_j. \qquad (60)$$

Thus, the lifetime of a quadruply excited level is given by

$$\tau = \frac{1}{\sum_{j=10}^{12}\operatorname{Re}\lambda_j}. \qquad (61)$$

This somewhat counter-intuitive result indicates that the cascade falling down electrons spend ever less time on their orbits, simulating a sort of free fall motion. Note also that unlike the standard case when it is the largest Lyapunov exponent that matters only, we obtain the sum of three exponents here.

Some results obtained using the formulae (52), (57) with the condition (53) are given in Table 2. In Figure 8 we show a part of the energy spectrum for a number of N values. As can be seen from Figure 8 the vibronic contribution to the energy appears considerable, with the density of levels increasing as the continuum is approached.

Table 2. Semiclassical energy levels ($Z = 4$) with $N = 10$ and $\sum_k n_k \leq 2$ and estimated values for the corresponding decay widths.

N	n_1	n_2	n_3	n_4	n_5	E (au)	Γ (au)
10	0	0	0	0	0	−1.29935	0.506
10	0	0	0	0	1	−1.15414	0.424
10	0	0	0	0	2	−1.03198	0.359
10	0	0	0	1	0	−1.12244	0.407
10	0	0	0	1	1	−1.00514	0.345
10	0	0	0	2	0	−0.97934	0.331
10	0	0	1	0	0	−1.10970	0.400
10	0	0	1	0	1	−0.99434	0.339
10	0	0	1	1	0	−0.96895	0.326
10	0	0	2	0	0	−0.95872	0.321
10	0	1	0	0	0	−1.08604	0.387
10	0	1	0	0	1	−0.97425	0.329
10	0	1	0	1	0	−0.94963	0.316
10	0	1	1	0	0	−0.93970	0.312
10	0	2	0	0	0	−0.92124	0.302
10	1	0	0	0	0	−1.07814	0.383
10	1	0	0	0	1	−0.96754	0.325
10	1	0	0	1	0	−0.94316	0.313
10	1	0	1	0	0	−0.93334	0.308
10	1	1	0	0	0	−0.91507	0.299
10	2	0	0	0	0	−0.90895	0.296

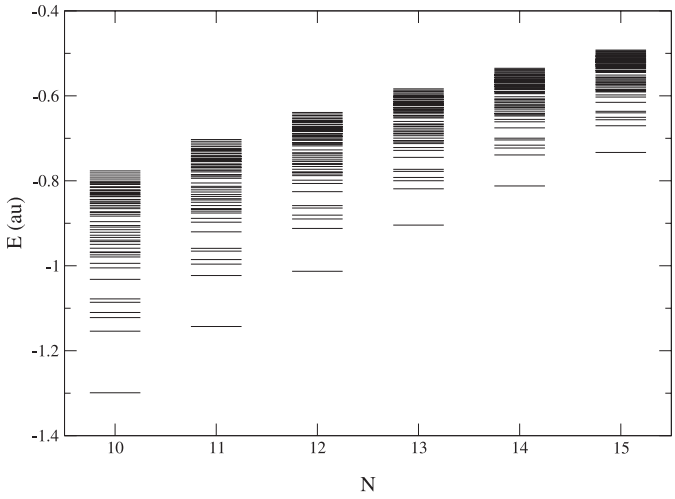

Fig. 8. The part of semiclassical energy spectrum ($Z = 4$) which contains the levels with $N = 10, ..., 15$ and $\sum_k n_k \leq 3$.

5 Conclusions

The extension from the triply to quadruply excited states turns out nontrivial. First, the number of possible underlying classical configurations raises considerably. We have restricted ourselves in this paper to one of the most simple plane models, but even in this case the spectrum appears very complex.

Of course, four equivalent electrons obviously violate Pauli's principle, but in real highly excited states two pairs of equivalent electrons are practically indistinguishable from the four particles intrashell. One may consider the system as composed of two equivalent electrons with opposite spins and with $L = L_{max}/2$, and another pair with $L = (L_{max}-1)/2$, both practically with circular, mutually indistinguishable orbits (see, e.g. [4] for the equivalent quantum mechanical situation).

If the present results are to be compared with the relevant quantum mechanical ones, what in the absence of experimental data appears the only criterion for valuing the procedure employed, one must bear in mind that the two approaches are complementary. First, full quantum mechanical calculations are still feasible for the low lying states only, where the semiclassical approach is not expected to work. Second, the restricted model calculations, like those within the frozen-r approximation, are still of qualitative nature, aiming mainly at classifying possible quantum states. In this respect, semiclassical modeling can be helpful in choosing underlying configurations that may be used for the quantum mechanical calculations. How much effective this approach can be is well illustrated by the theory of near-threshold fragmentation, which has been based on the purely classical model due to Wannier.

As mentioned above experimental situation appears promising in the case of multiply excited low-lying states. As for the highly multiply excited states, including fourfold ones, they do not appear close neither from the experimental, nor from the quantum mechanical point of view (see, e.g. [14] for the latter perspective). In principle one may envisage various ways to produce experimentally fourfold excitations. One way would be that already used for the doubly and triply excited beryllium, as reported by [1]. Another procedure, also used by experimentalists, would involve multiple charge transfer between highly ionized atoms and neutrals in plasma. (We are indebted to the referee for drawing our attention to this point.) But the principal problem with identifying those multiply excited states is the nature of the spectrum which should result from these energy states. This problem has been successfully overcome in the case of the molecular rovibronic spectra, and hopefully may be equally well resolved in the case of atomic systems. The problem is, of course, closely related to the issue of the existence of other possible classical configurations, in addition to the one studied here. It is only after examining all other possible candidates that one can estimate the statistical weight of the present model. We envisage further studies of the issue.

Generally, highly excited states belong to the correspondence principle domain and can serve as tools for elucidating many quantum mechanical features of the atomic systems via a more transparent semiclassical models. Calculations presented in this paper should hopefully contribute to this end.

This work has been supported by the Ministry of Science and Environment Protection of Serbia.

References

1. S. Hasegawa, F. Yoshida, L. Matsuoka, F. Koike, S. Fritzsche, S. Obara, Y. Azuma, T. Nagata, Phys. Rev. Lett. **97**, 023001 (2006)
2. H. Nagaoka, Bull. Math. Phys. Soc. Tokyo **2**, 140 (1904)
3. J.W. Nicholson, Month. Not. Roy. Astr. Soc. **72**, 49 (1912)
4. Bao Cheng-guang, Phys. Rev. A **47**, 1752 (1993)
5. Bao Chengguang, Duan Yiwu, Phys. Rev. A **49**, 818 (1994)
6. C.G. Bao, J. Phys. B **25**, 3725 (1992)
7. C.G. Bao, Phys. Lett. A **250**, 123 (1998)
8. C. Nicolaides, N. Pianos, Y. Komninos, Phys. Rev. A **48**, 3578 (1993)
9. Y. Komninos, C. Nicolaides, Phys. Rev. A **50**, 3782 (1994).
10. L. B. Madsen, J. Phys. B. **36**, R223 (2003)
11. P. Grujić, Eur. Phys. J. D **6**, 441 (1999)
12. M. Poulsen, P. Madsen, Phys. Rev. A **72**, 042501 (2005)
13. M. Poulsen, P. Madsen, Phys. Rev. A **71**, 062502 (2005)
14. T. Morishita, C.D. Lin, Phys. Rev. A **71**, 012504 (2005)
15. M. Walter, J.S. Briggs, J.M. Feagin, J. Phys. B. **33**, 2907 (2000)
16. L.B. Madsen, K. Molmer, Phys. Rev. A **64**, 060501(R) (2001)
17. L.B. Madsen, K. Molmer, Phys. Rev. A **65**, 022506 (2002)
18. P. Grujić, J. Phys. B **21**, 63 (1988)
19. N. Simonović, Phys. Rev. A **50**, 4390 (1994)
20. N. Simonović, M. Predojević, V. Panković, P. Grujić (unpublished)
21. S. Cvejanović, Z.D. Dohčević, P. Grujić, J. Phys. B **23**, L167 (1990)
22. P. Grujić, *X Eur. Symp. Dyn. Few-Body Sys.*, Balatonfuüred, 1986, edited by Gy. Bencze, P. Doleshall, J. Reval (Budapest, 1986), pp. 253–281
23. N. Simonović, P. Grujić, in *Adv. Math. Study of Atomic Doubly-Excited States*, Medellin, Colombia, 1995, edited by J. Mahecha, J. Botero (Universidad de Antioquia, 1996), pp. 107–153
24. Y. Kuchiev, V. Ostrovsky, Phys. Rev. A **58**, 321 (1998)
25. G.H. Wannier, Phys. Rev. **90**, 817 (1953)
26. N. Norcliffe, in *Case Studies in Atomic Physics*, Vol. 4, edited by W. McDaniel, M.R.C. McDowell (North-Holland, Amsterdam, 1975), pp. 45-55
27. A.F. Ozorio de Almeida, *Hamiltonian Systems: Chaos and Quantization* (Cambridge University Press, New York, 1992)
28. L. Landau, E. Lifshitz, *Quantum Mechanics* (Pergamon Press, Oxford, 1965)
29. P. Grujić, J. Phys. B **16**, 2567 (1983)
30. H. Goldstein, *Classical Mechanics* (Addison-Wesley, London, 1981)
31. I.M. Gel'fand, *Lectures in Linear Algebra* (Nauka, Moscow, 1966) (in Russian)
32. N.S. Simonović, J. Chem. Phys. **124**, 014108 (2006)
33. N.S. Simonović, J.M. Rost, *Classical Lifetimes for Quantum Resonances*, Twenty Second International Conference on Photonic, Electronic, and Atomic Collisions (XXII ICPEAC), Abstracts of Contributed Papers, edited by S. Datz, M.E. Bannister, H.F. Krause, L.H. Saddiq, D.R. Schultz, C.R. Vane (Rinton Press, 2001), p. 212